



OPEN Sodium butyrate promotes synthesis of testosterone and meiosis of hyperuricemic male mice

Jiaojiao Qi¹, Yu Sun¹, Zeqing Chen^{3,4,5}, Ruipeng Gao¹, Miao Song¹, Tong Zou¹, Xuelin Gong¹, Shuang Wang¹, Qing Zhang¹, Chengyang Liu¹ & Shichao Xing^{1,2}✉

Hyperuricemia (HUA) impairs spermatogenesis. This study was carried out, aiming to determine whether butyric acid (NaB) avoids the HUA-induced decline of sperm quality. HUA mice were developed through intra-peritoneal injection of the potassium oxalate combined with intragastric uric acid (UA) and by tube feeding 300 mg·kg⁻¹·d⁻¹ NaB. The effect of NaB on the reproduction of HUA male mice was determined by measuring sperm count, sperm motility and testosterone content. In addition, TM3 and GC-2 cells were treated with a solution containing 30 mg/dl UA and 1mM NaB. The effects of NaB on the sperm quality were evaluated with the expression level of the genes involving in LH/cAMP/PKA signaling pathway and meiosis, and that encoding OPRL1 receptor protein. Results showed that NaB improved sperm count, sperm motility, testosterone synthesis, and impaired spermatocyte meiosis *via* HUA. In addition, *in vitro* analysis showed that NaB activated the LH/cAMP/PKA signaling pathway of TM3 cells, promoted the synthesis of testosterone, up-regulated the content of pain-sensitive peptide receptor (OPRL1) on the surface of GC-2 cells, and promoted meiosis. NaB also promoted the utilization of ATP by GC-2 cells. We illustrated a close relationship between HUA and spermatogenesis defects. NaB-promoted the expression of the genes functioning in testis meiosis, and the testosterone content may aid to improving spermatogenesis quality.

Keywords Hyperuricemia, Sodium butyrate, Sperm quality, Testosterone, Meiosis

Abbreviations

HUA	Hyperuricemia
UA	Uric acid
SCFA	Short-chain fatty acid
NaB	Sodium butyrate
N/OFQ	Nociceptin/orphanin-FQ
GnRH	Gonadotropin-releasing hormone
T	Testosterone
FSH	Follicle-stimulating hormone
LH	Luteinizing hormone

Hyperuricemia (HUA) is a metabolic disease caused by the imbalance of uric acid (UA) metabolism¹. In China, the prevalence of HUA among adolescents is increasing annually with a discomfort spreading trend toward the people at young ages. It has now emerged as the second most common metabolic disorder after diabetes^{2,3}. Statistics has showed that 55.8 million people worldwide are suffering from gout in 2020, and the prevalence of gout in men is 3.26 times higher than that in women. The total number of gout cases may reach 95.8 million by 2050⁴. Previous studies have demonstrated that metabolic disorders frequently lead to fertility decline⁵. HUA can impact male reproductive ability in several ways. It may alter the sex hormone level, hindering the maturation and development of sperm. It may also intensify the oxidative stress, contributing to sperm dysfunction^{6,7}. However, less studies have been carried out on the mechanism underlining such influence. The limited studies includes one carried out in our laboratory, which demonstrated that HUA mice exhibit testicular tissue damage and degenerated sperm quality.

¹Department of Pathogen Biology, College of Basic Medicine, Qingdao University, Qingdao 266071, P. R. China.

²Women and Children's Hospital, Qingdao University, Qingdao 266075, P. R. China. ³Municipal Center for Disease Control and Prevention of Qingdao, Qingdao 266033, China. ⁴Qingdao Municipal Hospital, Qingdao 266000, Shandong, China. ⁵Medical Integration and Practice Center, Shandong University, Jinan 250012, China. ✉email: xingshichao@qdu.edu.cn

Short-chain fatty acids (SCFAs), the primary metabolism products of dietary fiber in the colon, play a crucial role in the complex interaction between host diet and gut microorganism⁸. Acetate, propionate and butyrate are the most commonly found SCFAs in human body, which are the predominant short-chain fatty acids in the colon⁹. Studies have demonstrated that sodium butyrate (NaB) supports probiotic flora and safeguard the intestinal barrier^{10,11}. In Uox knockout mice with elevated uric acid level, the number of bacteria that produce SCFAs significantly increased, leading to a low concentration of SCFAs¹². The depletion of butyric acid-producing bacteria and the decrease in NaB content were particularly pronounced in HUA mice^{13,14}. In addition, *Clostridium butyricum* and NaB have been shown to ameliorate testicular injury in rats¹⁵. However, the relationship between NaB and the quality of sperm against the background of HUA is not clear.

In this study, we examined the association of pathogenesis of NaB with sperm quality against the background of HUA, and investigated the processes of testosterone synthesis and spermatogenesis by constructing a HUA mouse model and using TM3 Leydig cell line and GC-2 cell line. TM3 Leydig cell line is widely used in studying male reproductive endocrinology, particularly the synthesis and secretion of testosterone while GC-2 is widely used in investigating spermatogenesis and related molecular mechanisms. Our study was a novel trial of treating HUA and its complications, which should aid to developing new clinical drugs.

Materials and methods

Animals

Eighteen 7-week-old male SPF C57BL/6 mice, 22 ± 4 g in body weight, were purchased from Jinan Pengyue Co., Ltd. After being acclimatized for 7 days, they were used in an in vivo study. The mice individuals were divided into three groups, a control group (CON, $n=6$), a hyperuricemia group (HUA, $n=6$) and a sodium butyrate treatment group (HD, $n=6$). The HUA and HD groups received daily intraperitoneal injections of potassium oxalate ($250 \text{ mg} \cdot \text{kg}^{-1}$) and intragastric administration of uric acid ($200 \text{ mg} \cdot \text{kg}^{-1}$) simultaneously. The uric acid was purchased from Sangon Biotech Co., Ltd., which was dissolved in 0.5% CMC-Na (Sangon Biotech Co., Ltd.)^{16,17}. The CON group was subcutaneously injected with normal saline, $0.1 \text{ mL}/10 \text{ g}$, and then administrated 0.5% CMC-Na with gavage. In the third week, the HD group was supplemented with $300 \text{ mg}/(\text{kg} \cdot \text{d})$ NaB solution (Shanghai Macklin Biochemical Technology Co., Ltd. (Fig. S1). In the sixth week^{18,19}, all mice individuals were sacrificed with isoflurane anesthetic with blood and testicular tissue sampled for analysis.

Our animal study was reviewed and approved by the Animal Research Ethics Committee of the Affiliated Hospital of Qingdao University (Approval code: AHQU-MAL20230322). All operations followed the relevant guidelines and regulations detailed in ARRIVE guidelines.

Cell lines

The mouse Leydig cells (TM3) and the mouse spermatocytes (GC-2) were obtained from the Cell Bank of Shanghai, Chinese Academy of Sciences. TM3 cells were maintained in DMEM/F12 (Procell Life Science & Technology Co., Ltd) supplemented with 5% horse serum (Procell Life Science & Technology Co., Ltd) and 2.5% fetal bovine serum (Procell Life Science & Technology Co., Ltd). GC-2 cells were cultured in DMEM (Procell Life Science & Technology Co., Ltd) supplemented with 10% fetal bovine serum (Procell Life Science & Technology Co., Ltd). Both cell lines were divided into CON, HUA and HD groups, treated with 1 mM NaB or $30 \text{ mg}/\text{dL}$ UA accordingly with the total cellular proteins and mRNA extracted after 24 h ^{20–22} (Fig. S2).

Sperm counting

The tail of the epididymis was collected and divided into several sections. The epididymis and vas deferens were gently squeezed using ophthalmic tweezers. Sperms were extracted into the physiological saline while the epididymis and vas deferens were removed after extraction. The sperms were incubated at 37°C and 5% CO_2 and in saturated humidity for 10 min to promote dispersion. Semen was then absorbed with an eyedropper and placed at the junction between the counting chamber of the blood cell counting plate (Shanghai QiuJing Biochemical Reagent Instrument Co., Ltd.) and coverglass (Thermo Fisher Scientific Inc). To calculate the sperm density, the total number of sperms in five central squares including four corners and middle one were counted. According to the third-grade sperm motility score (PR, NP, IM) outlined in the fifth edition of the WHO guidelines, the sperm motility was determined by summing the forward movement (PR) and non-forward movement (NP).

Immunohistochemistry and Immunofluorescence analyses

Testicular tissue slices were placed in an antigen repair buffer (pH 6.0) for antigen retrieval. The discs were then immersed in 3% of hydrogen peroxide (Servies, Wuxi, China), and incubated at room temperature in dark for 25 min to block endogenous peroxidase activity. The tissue was then uniformly covered with 3% BSA (Servies, Wuxi, China) and incubated at room temperature for 30 min. The primary antibodies, steroidogenic acute regulatory protein (STAR), luteinizing hormone receptor (LHR), cytochrome P450 family 11 subfamily A member 1 (CYP11A1) and opioid-related nociceptin receptor 1 (OPRL1) (1:200, Affinity), were added and incubated at 4°C overnight. A secondary antibody (1:5000, Affinity) was added, incubated at room temperature for 50 min. After washing and gently drying, the freshly prepared DAB color developer (Servies, Wuxi, China) was added with the color development monitored under a microscope. The positive staining should appear in brown and yellow. The cellular nuclei were counterstained, dehydrated, sealed, and examined under a microscope (Nikon E100) with the image collected and analyzed.

The testicular tissue sections were treated with 50–100 μL membrane-disrupting working solution (Servies, Wuxi, China), uniformly covered with 3% BSA (Servies, Wuxi, China) and incubated at room temperature for 30 min. The primary antibodies, proliferating cell nuclear antigen (PCNA), receptor tyrosine kinase (c-Kit) and WT1 transcription factor (WT-1) (1:200, Affinity), were added and incubated at 4°C overnight, and then

at room temperature for 50 min when mixed with a fluorescent secondary antibody (1:100, Affinity). Nuclei were stained with DAPI (Servies, Wuxi, China). The stained were sealed and examined under a fluorescence microscope (Nikon E100) with images collected.

Intracellular Cyclic adenosine monophosphate (cAMP) and protein kinase A (PKA) detection

The suspension of cells were diluted with PBS (Procell Life Science & Technology Co., Ltd) at acidities varying between pH7.2 and pH7.4 into approximately 1 million cells per milliliter. Ultrasonic waves were used to disrupt the cells and release intracellular constituents. The mixture was centrifuged at 4 °C and 2,000 to 3,000 rpm for about 20 min with the supernatant used for ELISA detection (Elabsience Biotechnology Co., Ltd). The supernatant was carefully collected and used to BCA (Yatase, Shanghai, China) analysis of proteins. The absorbance measured was proportional to the content of cAMP and the activity of PKA, respectively. For reliable results, the total amount of protein per histone was consistent.

Biochemical parameter analysis

The uric acid content in serum was measured using a uric acid detection kit (NJJC BIO). The ELISA kit (Elabsience Biotechnology Co., Ltd) was used to assess the serum concentrations of hormones including nociceptin/orphanin-FQ (N/OFQ), gonadotropin-releasing hormone (GnRH), luteinizing hormone (LH), follicle-stimulating hormone (FSH) and testosterone. Additionally, other kits (Elabsience Biotechnology Co., Ltd) were utilized to determine the concentrations of Ga^{2+} and reactive oxygen species (ROS), the activity of ATPase, the mitochondrial membrane potential, and the abundance of other intracellular proteins.

Western blotting analysis

Protein was extracted from tissues or cells using RIPA buffer (Beyotime, Shanghai, China) with protein concentration determined using the BCA assay kit (Yatase, Shanghai, China). After uniform loading, the standard Western blotting analysis was carried out. The following antibodies were utilized, which included LHR, STAR, CYP11A1, OPRL1 and GAPDH (1:1000, Affinity).

Quantitative real-time PCR (qPCR)

TRIzol reagent (Thermo Fisher Scientific Inc) was used to isolate total RNA from tissues and cells following manufacturer's instructions. The RNA was reversely transcribed into complementary DNA (cDNA). Amplification was performed on the LightCycler 480 Instrument II.

Statistical analysis

The data were assured to be normally distributed. The independent *t*-test was used to determine the significance of the difference between two groups. One-way ANOVA was utilized to test the significance of the difference among groups. The Tukey method was applied for post-hoc analyses. For the data departing from the normal distribution, a non-parametric test (Kruskal-Wallis test) was conducted. All data are expressed as mean \pm standard deviation. GraphPad Prism 9.5 was used to generate figures. SPSS 20.0 was employed for data processing. A difference was believed to be statistically significant if $p < 0.05$ and very significant if $p < 0.01$.

NaB improved sperm quality and increased hormone level in HUA mice

NaB enhanced sperm motility and increased sperm count in mice with HUA

To verify the protective effect of NaB against the background of HUA on sperm quality, we developed an HUA model mice, and administered them NaB solution. At week 6, the body weight of HUA group was found to be lower than that of CON and HD groups (Fig. 1a) while the serum uric acid level of HUA group was significantly higher than that of CON and HD groups (Fig. 1b). The sperm count and motility of HUA group reduced significantly although there was no notable difference in the testicular coefficient (Fig. 1c and e). A decrease in the coefficient implied that the testicular development is inhibited or the function of testis is impaired while an increase in the coefficient indicated that the proliferation is abnormal. HE staining revealed a significant reduction in spermatogenic cells within the seminiferous tubules of HUA group (Fig. 1f). In contrast, all measured indices of HD group showed a significant recovery compared to HUA group. NaB improved the sperm quality when the function of testis was impaired by HUA.

NaB regulates the contents of serum testosterone, LH, FSH and GnRH of mice with HUA

To investigate the effect of NaB on hyperuricemic sex hormones, we examined the levels of serum GnRH, testosterone, FSH and LH. As illustrated in the Fig. 2, the serum level of testosterone of HUA group decreased (Fig. 2d) while that of FSH increased significantly (Fig. 2c). In contrast, the serum levels of GnRH and LH remained unchanged (Fig. 2a and b). Of HD group, the testosterone level increased (Fig. 2d), and that of FSH returned to the normal (Fig. 2c). These observations suggested that NaB regulated the serum hormone level of HUA mice, and increased the serum level of testosterone.

NaB activated LH/cAMP/PKA signaling pathway, promoting testosterone synthesis

To further investigate the mechanism underlining NaB promotion to testosterone synthesis of HUA mice, we focused on the LH/cAMP/PKA signaling pathway, a well-established pathway towards testosterone synthesis in Leydig cells²². We assessed the expression levels of LHR, STAR and CYP11A1 genes in both testicular and stromal cells. The protein content of LHR, STAR and CYP11A1 and the transcript abundance of their genes in testicular tissue were significantly reduced in HUA group (Fig. 3a and d). The number of Leydig cells in HUA group was lower than that in CON and HD groups as was indicated by red arrow (Fig. 3a). The findings in vitro TM3 cells corroborated the findings from tissues (Fig. 3e and k). The levels of cAMP and PKA protein in TM3

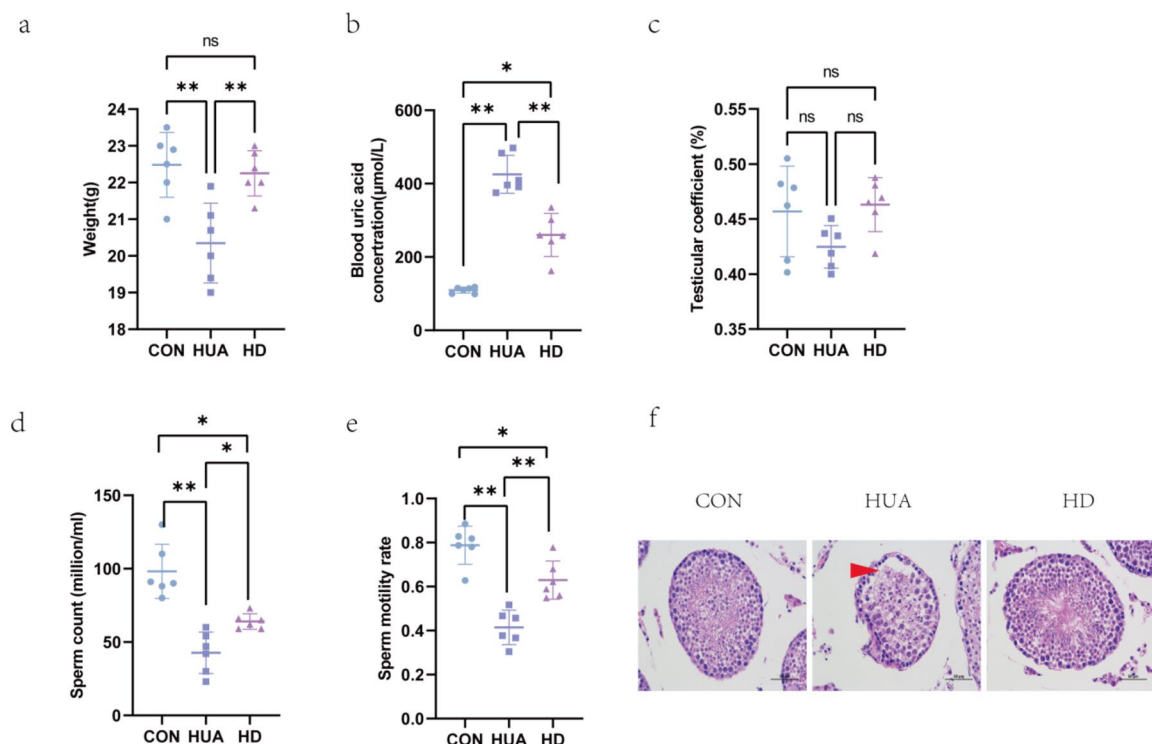


Fig. 1. The investigation of the reproductive toxicity and protective effect of NaB against HUA background in male mice. (a), weight change of the mice; (b), serum uric acid concentration ($n=6$); (c), testicular coefficient (testicular weight/ weight $\times 100\%$, $n=6$); (d), sperm count ($n=6$); (e), sperm motility rate ($n=6$); (f), testicular structure examined after hematoxylin and eosin staining (arrows pointing to the abnormal structures, the decrease of spermatogenic cells). Data are presented as mean \pm standard deviation. *, $p < 0.05$; **, $p < 0.01$. Scale bar = 50 μ m.

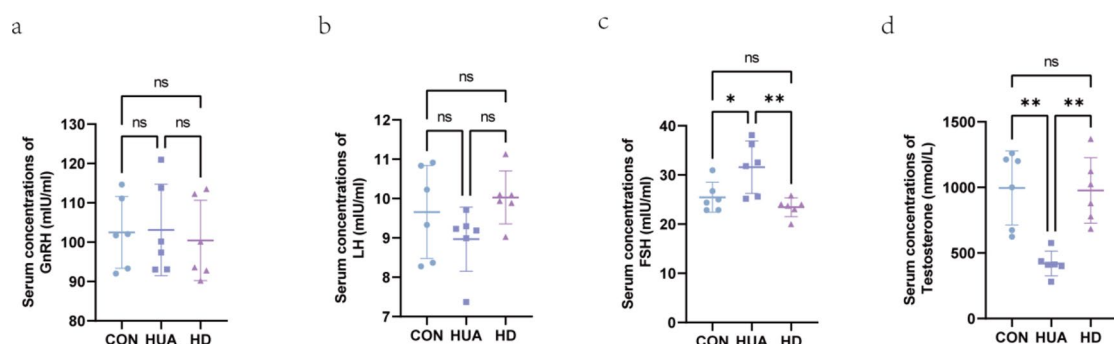


Fig. 2. The effects of HUA and NaB on serum testosterone, GnRH, LH, and FSH levels. The concentrations of GnRH (a), LH (b), FSH (c) and testosterone (d) in serum were quantified using ELISA, and expressed as mean \pm SD. *, $p < 0.05$; **, $p < 0.01$.

cells decreased when the concentration of uric acid is high (Fig. 3l and m). In HD group, the syntheses of cAMP, PKA and testosterone were elevated (Fig. 3l and n). These findings suggested that NaB enhanced testosterone production by modulating the LH/cAMP/PKA signaling pathway.

NaB improved the sperm production of function-impaired testis

NaB promoted the spermatocyte meiosis of HUA mice

To decipher the mechanism underlying the sperm production of the function-impaired testis of HUA group, the proliferation of spermatogonium and spermatocyte was detected by PCNA proliferating cell nuclear antigen fluorescent staining. The results showed that the numbers of spermatogonia and spermatocytes of HUA group were lower than those of CON and HD groups (Fig. 4a and b). In addition, the differentiation of spermatogonia was evaluated with c-Kit. We found a high average fluorescence area in HUA group (Fig. 4c and d).

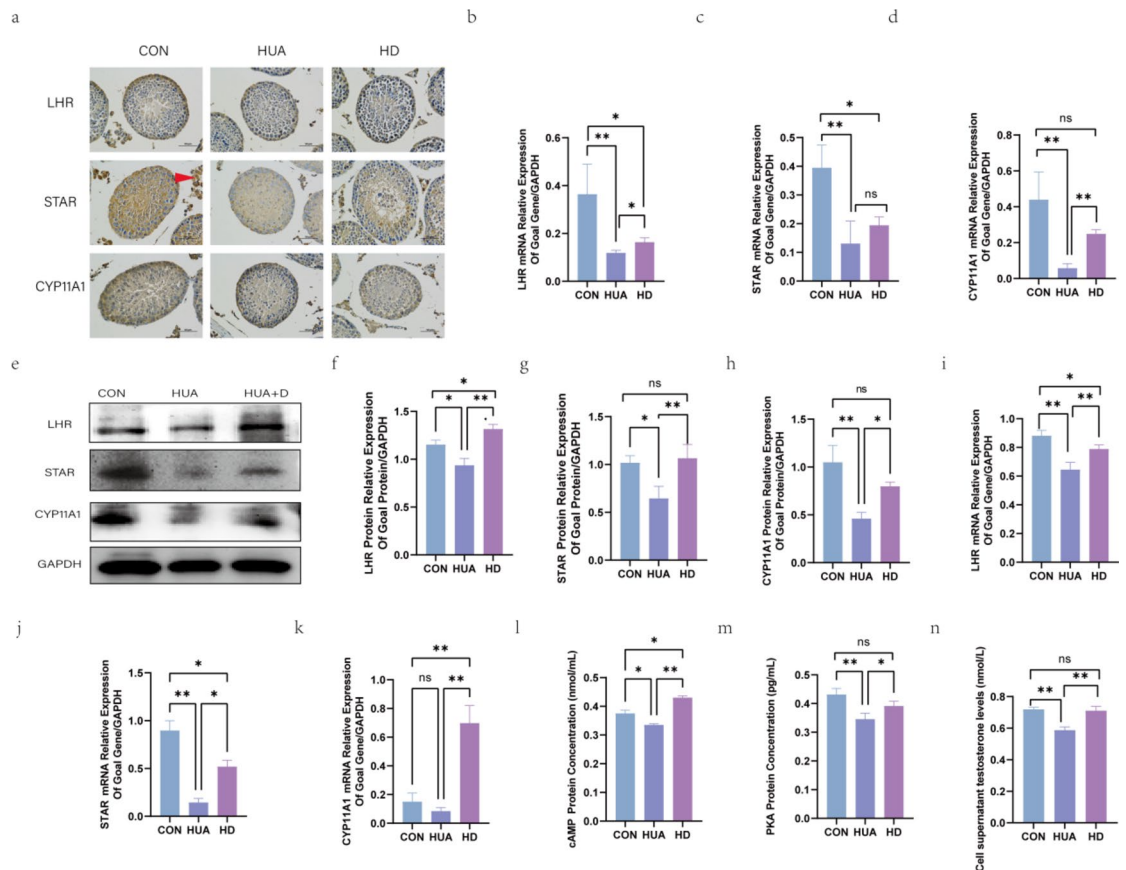


Fig. 3. NaB up-regulates the expression of LHR, CYP11A1s, and STAR proteins and genes in testis. (a), the expression levels of LHR, CYP11A1 and STAR proteins in testicular tissue; (b), (c) and (d), the transcript abundances of these genes in testicular tissue; (e), (f), (g) and (h), the protein contents of LHR, STAR and CYP11A1 in TM3 cells ($n = 3$); (i), (j) and (k), the transcript abundances of LHR, STAR and CYP11A1 genes in TM3 cells; (l), (m) and (n), the concentrations of intracellular cAMP, PKA and testosterone in the cell supernatant. Data are presented as mean \pm SD. *, $p < 0.05$, **, $p < 0.01$. Scale bar = 50 μ m. The arrows denote testicular interstitial cells.

These observations demonstrated that HUA facilitated the differentiation of spermatogonia into spermatocytes; however, meiosis in spermatocytes was inhibited, leading to a reduction in spermatogenesis.

NaB promoted the expression of meiosis-related genes in spermatocytes against high uric acid background

NaB influenced the meiosis pathway of spermatocytes against HUA background in mice. Immunofluorescence detection of WT-1, a signature antibody for Sertoli cells, revealed that three groups are not different significantly (Fig. 5a and c). Serum level of nociceptin/orphanin-FQ (N/OFQ) of HUA group was lower than that of CON and HD groups. HD group exhibited an elevation of N/OFQ level (Fig. 5f). The level of OPRL1 (opioid-related nociceptin receptor 1) in the testes of HD group was higher than that of HUA group (Fig. 5a and b). The trend of OPRL1 gene expression in GC-2 cells was consistent with that found in animals (Fig. 5d and e). The expression level of meiosis-related genes including *Dmc1*, *Stra8* and *Hspa1b* and those encoding several structural maintenance of chromosome (SMC) proteins (*Smc1b*, *Smc4*, *Smc5*) and synaptic complex proteins (*Sycp1*, *Sycp2*) was analyzed using qPCR. The HUA group exhibited lower expression levels compared to CON and HD groups (Fig. 5g). NaB promoted the synthesis of N/OFQ and the expression of meiosis-related genes.

NaB improved the energy supply in GC-2 cells in high uric acid environment

To decipher whether NaB improves the utilization of ATP and reduces the level of oxidative stress, we determined the fluorescence intensity of the JC-1 polymer/monomer of HD group. We found that mitochondrial function is impaired in the HUA group (Fig. 6a and c). In addition, the level of reactive oxygen species of HUA group was elevated compared to that of HD group (Fig. 6b and d). Intracellular measurements of Ca^{2+} , cAMP, PKA and ATPase indicated that the levels of Ca^{2+} , cAMP, PKA and ATPase activity of HUA group were significantly lower than that of CON and HD groups (Fig. 6b and h). These findings suggested that NaB inhibited the cellular oxidative stress, and improved the mitochondrial function of spermatocytes, and enhanced ATP utilization.

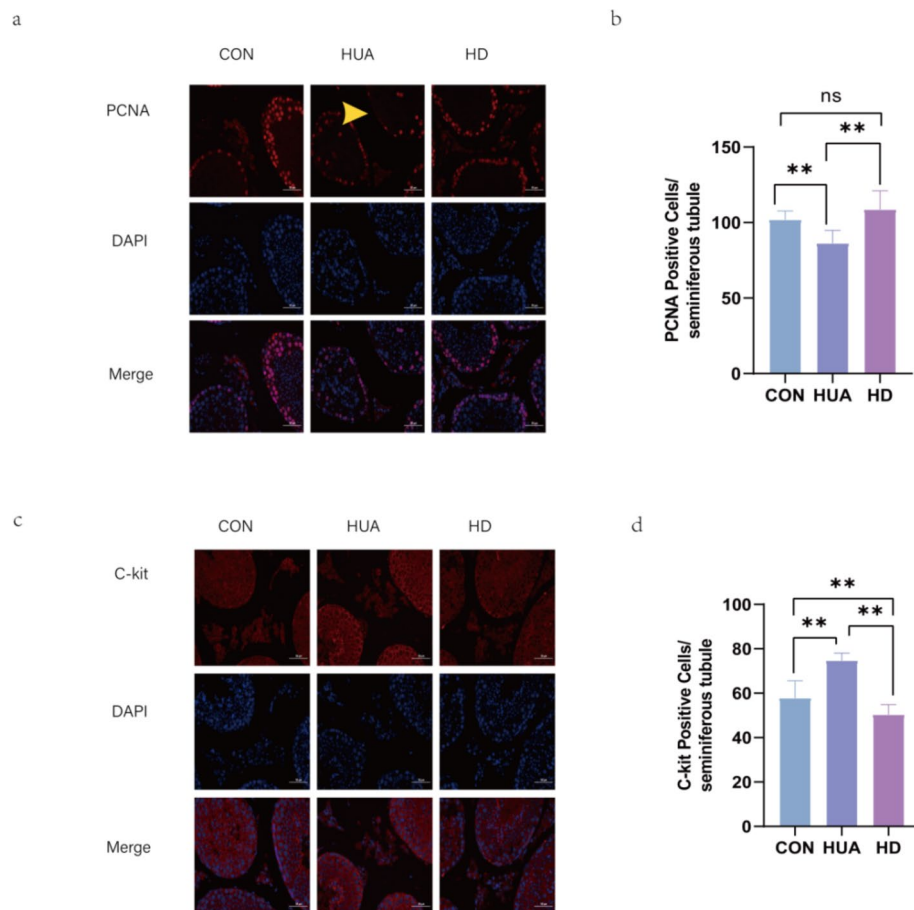


Fig. 4. NaB enhances the meiosis of HUA mice. **(a)** and **(c)**, the expression levels of PCNA and c-Kit protein in testicular tissue. The testicular tissue was stained with PCNA and c-Kit (red) and DAPI (blue). c-Kit play an important role in the development and differentiation of spermatogenic cells. Undifferentiated spermatogonia do not express c-Kit, but are expressed in differentiated spermatogonia, so it can be used as an indicator of whether spermatocytes are differentiated. Spermatogenic cells (spermatogonia and spermatocytes) in HUA group exhibits a diminished capacity of proliferation (scale = 50 μ m) (arrows indicated). **(b)**, **(d)**, the expression levels of PCNA and c-Kit protein as was quantified using ImageJ ($n = 3$). Data are expressed as mean \pm SD. *, $p < 0.05$; **, $p < 0.01$.

Discussion

In this study, we developed a HUA mouse model to investigate the relationship among NaB, HUA and sperm quality. Our findings indicated that NaB enhanced the sperm quality in HUA mice.

Previous studies have shown that NaB contributes to the excretion of uric acid and exhibits protective effects including anti-inflammatory and antioxidant properties^{10,23–25}. The uric acid level of HUA group was significantly higher than that of HD group while the body weight of HUA group was lower than that of CON and HD groups. The improvement of sperm quality and weight change have been observed in HUA mice, which may associate with the protective effect. During testosterone synthesis, two hormones, FSH and LH, are primarily released by the pituitary gland and move to testes *via* bloodstream. FSH initiates sperm production whereas LH stimulates testosterone production in Leydig cells^{22,26,27}. Low testosterone level in body inhibits the process of sperm production²⁸. We found that the hormone level of HUA group changed significantly. Testosterone level decreased while FSH level increased. No difference in GnRH and LH levels was observed. The LH/cAMP/PKA signaling pathway is a well-established pathway that regulates testosterone synthesis²⁹. Previous studies have found that activation of the cAMP/PKA signaling pathway enhances testosterone synthesis in Leydig cells²². We found that Leydig cells reduced in HUA group, and the levels of LHR, STAR protein and CYP11A1 proteins reduced as well. NaB was found to upregulate the levels of LHR, STAR, and CYP11A1 proteins, and increase the number of Leydig cells in HD group. HUA not only affects the quantity of Leydig cells but also impairs testosterone synthesis by reducing LHR and enzymes related to steroid hormone synthesis. To further investigate the effects of HUA and NaB on testosterone synthesis, TM3 cell experiments were conducted. The levels of testosterone, LHR, cAMP, PKA, STAR and CYP11A1 of HUA group were found to be lower than those of HD group, which corroborated the findings from animal experiments. These results suggested that NaB promotes testosterone synthesis by upregulating LHR protein levels and activating the cAMP/PKA signaling pathway.

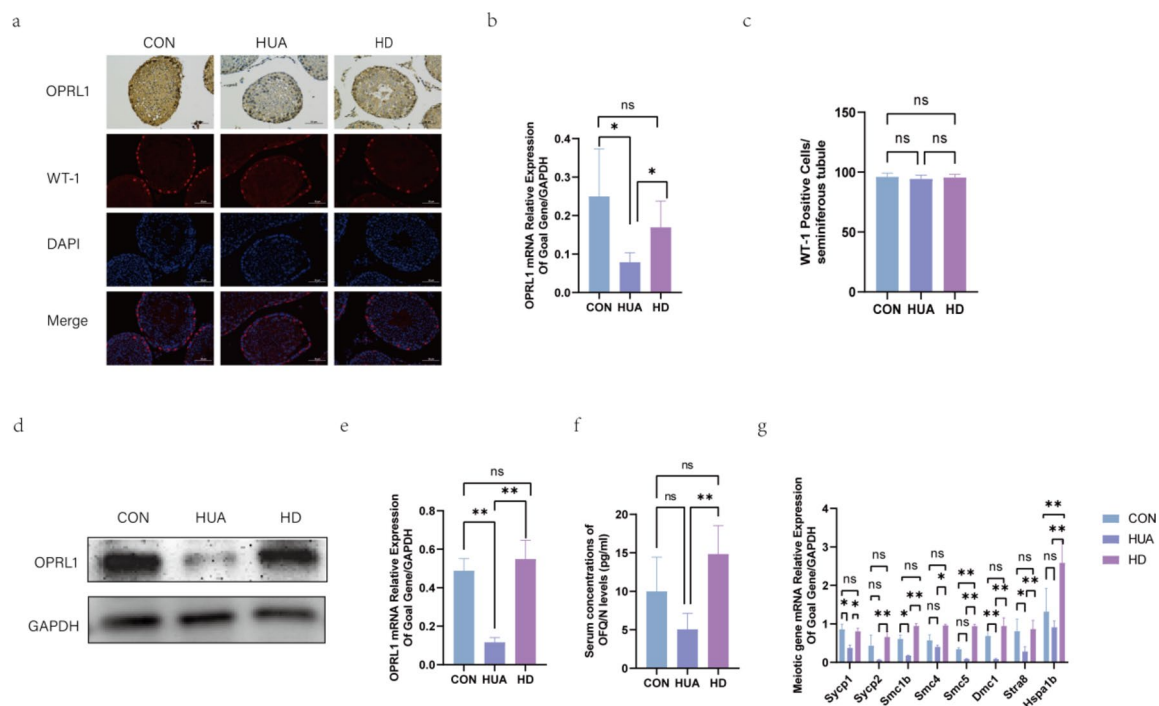


Fig. 5. NaB promotes the secretion of N/OFQ and increases the expression of genes associated with meiosis in spermatocytes. (a), the immunohistochemical detection of OPRL1 (N/OFQ receptor) and the immunofluorescence detection of WT-1 in testicular tissue. (b), and (c), the expression level of OPRL1 and WT-1 genes ($n = 6$). (d), (e) and (f), the serum level of N/OFQ. (g), the transcript abundances of meiosis-related genes, *Smc1b*, *Smc4*, *Smc5*, *Sycp1*, *Sycp2*, *Dmc1*, *Stra8*, *Hspa1b*, in spermatocytes. Data are expressed as mean \pm SD. *, $P < 0.05$; **, $P < 0.01$. The scale bar = 50 μ m.

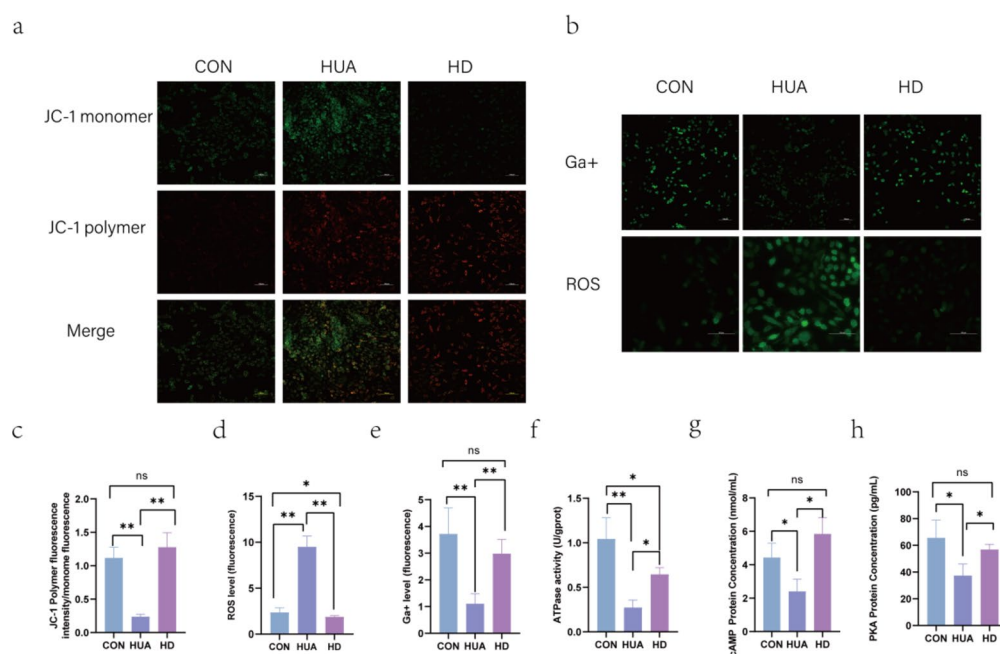


Fig. 6. NaB improves ATP utilization and diminishes the level of oxidative stress. (a), (b), the mitochondrial membrane potential, ROS and Ga^{2+} levels. (c), (d) and (e), the expression levels of the mitochondrial membrane potential, ROS and Ga^{2+} as quantified using ImageJ ($n = 3$). (f), the ATPase activity in GC-2 cells. (g) and (h), the level of cAMP and PKA in GC-2 cells. The data are presented as mean \pm SD. *, $P < 0.05$; **, $P < 0.01$. The scale bar = 100 μ m.

We found that sperm count and sperm motility of HUA group were lower than those of HD group. Immunofluorescence detection of PCNA and c-Kit protein in testicular tissue indicated that the number of spermatogonia and spermatocytes of HUA group was substantially lower than that of CON and HD groups. High uric acid level promoted the differentiation of spermatogonia into spermatocytes, which was accompanied by the reduction in sperm count in HUA group, indicating that the meiosis of spermatocytes was inhibited. NaB promoted spermatocytes to complete meiosis when the concentration of uric acid is high and increased the number of spermatocytes. The entire meiosis occurs within the seminiferous tubules, which is regulated by Sertoli cell's secreted factors except for the genes of spermatogenic cells³⁰. Studies have shown that N/OFQ secreted by Sertoli cells acts on the OPRL1 receptor, influencing the separation of meiotic chromosomes, and thereby allowing meiosis to proceed normally^{31,32}. OPRL1 is synthesized in testicular tissue and localizes at the cell membrane of spermatocytes³². The number of Sertoli cells was similar among three groups. However, the serum N/OFQ content of HUA group was lower than that of HD group. The OPRL1 receptor content of GC-2 cells of HUA group was significantly lower than that of CON and HD groups. The expression of meiosis-related genes in HD group was higher than that in HUA group. These results indicated that NaB promotes meiosis by increasing serum N/OFQ levels and upregulating the OPRL1 receptor content on the surface of GC-2 cells.

Previous studies have shown that protein kinase A (PKA) catalyzes subunit deficiency in mice, ultimately leading to sterility^{33,34}. PKA, as a crucial substrate of the cAMP/PKA signaling pathway, is involved in sperm formation and maturation^{22,35,36}. Moreover, the cAMP-PKA signaling pathway regulates mitochondrial function and promotes mitochondrial Ca^{2+} accumulation^{37,38}. Ca^{2+} provides energy for cells by activating ATP synthetase in mitochondria, regulating mitochondrial phosphorylation, and promoting ATP synthesis and hydrolysis³⁹. The completion of this process requires the stability of the mitochondrial membrane potential; any alteration in this potential adversely affects ATP synthesis⁴⁰. A lack of adequate energy supply disrupts also the proper functioning of meiosis^{41–43}. In addition, mitochondrial calcium level changes with the maturation process of meiosis, and calcium homeostasis plays also a crucial role in meiosis^{44,45}. In the GC-2 cells, intracellular levels of Ca^{2+} , cAMP, PKA and ATPase of HUA group were lower than those of CON and HD groups. The expression of meiosis-related genes in HUA group was lower than that in CON and HD groups. These results demonstrated that NaB enhances mitochondrial function and ATP utilization in GC-2 cells, facilitating meiosis.

Conclusions

NaB enhanced testosterone synthesis and promoted the expression of meiosis-related genes in male mice with HUA, and reduced also the serum uric acid level. These findings provided new theoretical evidence supporting NaB applicability for treating HUA and its associating complications.

Data availability

All data generated or analysed during this study are included in this published article [and its supplementary information files]. And the datasets used and/or analysed during the current study available from the corresponding author on reasonable request.

Received: 9 December 2024; Accepted: 24 March 2025

Published online: 28 April 2025

References

- Yanai, H., Adachi, H., Hakoshima, M. & Katsuyama, H. Molecular biological and clinical Understanding of the pathophysiology and treatments of hyperuricemia and its association with metabolic syndrome, cardiovascular diseases and chronic kidney disease. *Int. J. Mol. Sci.* **22**, (2021).
- Li, Y. et al. Demographic, regional and Temporal trends of hyperuricemia epidemics in Mainland China from 2000 to 2019: a systematic review and meta-analysis. *Glob Health Action.* **14**, 1874652 (2021).
- Zhang, M. et al. Prevalence of hyperuricemia among Chinese adults: findings from two nationally representative Cross-Sectional surveys in 2015–16 and 2018–19. *Front. Immunol.* **12**, 791983 (2021).
- Global & national burden of gout. 1990–2020, and projections to 2050: a systematic analysis of the global burden of disease study 2021. *Lancet Rheumatol.* **6**, e507–e517 (2024).
- Carrageta, D. F. et al. Signatures of metabolic diseases on spermatogenesis and testicular metabolism. *Nat. Rev. Urol.* **21**, 477–494 (2024).
- Liu, Y. F. et al. Uncovering the potential mechanisms and effects of hyperuricemia and its associated diseases on male reproduction. *Reprod. Sci.* **31**, 2184–2198 (2024).
- Ma, J., Han, R., Cui, T., Yang, C. & Wang, S. Effects of high serum uric acid levels on oxidative stress levels and semen parameters in male infertile patients. *Med. (Baltim).* **101**, e28442 (2022).
- Li, Y. et al. Insoluble Fiber in Barley Leaf Attenuates Hyperuricemic Nephropathy by Modulating Gut Microbiota and Short-Chain Fatty Acids. *Foods* **11**, (2022).
- Rekha, K. et al. Short-chain fatty acid: an updated review on signaling, metabolism, and therapeutic effects. *Crit. Rev. Food Sci. Nutr.* **64**, 2461–2489 (2024).
- Chen, G. et al. Sodium butyrate inhibits inflammation and maintains epithelium barrier integrity in a TNBS-induced inflammatory bowel disease mice model. *EBioMedicine* **30**, 317–325 (2018).
- Zhong, H. et al. Sodium butyrate promotes Gastrointestinal development of preweaning bull calves via inhibiting inflammation, balancing nutrient metabolism, and optimizing microbial community functions. *Anim. Nutr.* **14**, 88–100 (2023).
- Guo, Y. et al. Inulin supplementation ameliorates hyperuricemia and modulates gut microbiota in Uox-knockout mice. *Eur. J. Nutr.* **60**, 2217–2230 (2021).
- Chu, Y. et al. Metagenomic analysis revealed the potential role of gut Microbiome in gout. *NPJ Biofilms Microbiomes.* **7**, 66 (2021).
- Martínez-Nava, G. A. et al. The impact of short-chain fatty acid-producing bacteria of the gut microbiota in hyperuricemia and gout diagnosis. *Clin. Rheumatol.* **42**, 203–214 (2023).
- Chen, Y. et al. The herb pair radix rehmanniae and cornus officinalis attenuated testicular damage in mice with diabetes mellitus through Butyric Acid/Glucagon-Like Peptide-1/Glucagon-Like Peptide-1 receptor pathway mediated by gut microbiota. *Front. Microbiol.* **13**, 831881 (2022).

16. Wen, S. et al. The Time-Feature of uric acid excretion in hyperuricemia mice induced by potassium oxonate and adenine. *Int. J. Mol. Sci.* **21**, (2020).
17. Dhoubi, R. et al. Creation of an adequate animal model of hyperuricemia (acute and chronic hyperuricemia); study of its reversibility and its maintenance. *Life Sci.* **268**, 118998 (2021).
18. Hussain, A. et al. *Limosilactobacillus reuteri* HCS02-001 Attenuates Hyperuricemia through Gut Microbiota-Dependent Regulation of Uric Acid Biosynthesis and Excretion. *Microorganisms* **12**, (2024).
19. Liu, X. et al. Commensal *Enterococcus faecalis* W5 ameliorates hyperuricemia and maintains the epithelial barrier in a hyperuricemia mouse model. *J. Dig. Dis.* **25**, 44–60 (2024).
20. Wu, D. L. et al. Study on the mechanism of Wuzi-Yanzong-Wan-mediated serum interfering with the mitochondrial permeability transition pore in the GC-2 cell induced by atractyloside. *Chin. J. Nat. Med.* **20**, 282–289 (2022).
21. Onorato, T. M., Brown, P. W. & Morris, P. L. Mono-(2-ethylhexyl) phthalate increases spermatocyte mitochondrial Peroxiredoxin 3 and cyclooxygenase 2. *J. Androl.* **29**, 293–303 (2008).
22. Jin, H. et al. Chronic exposure to polystyrene microplastics induced male reproductive toxicity and decreased testosterone levels via the LH-mediated LHR/cAMP/PKA/StAR pathway. *Part. Fibre Toxicol.* **19**, 13 (2022).
23. Li, Y. et al. Protective effect of sodium butyrate on intestinal barrier damage and uric acid reduction in hyperuricemia mice. *Biomed. Pharmacother.* **161**, 114568 (2023).
24. Liu, W. et al. Supplementation with sodium butyrate improves growth and antioxidant function in dairy calves before weaning. *J. Anim. Sci. Biotechnol.* **12**, 2 (2021).
25. Sarkar, A. et al. Butyrate limits inflammatory macrophage niche in NASH. *Cell. Death Dis.* **14**, 332 (2023).
26. Oduwale, O. O., Huhtaniemi, I. T. & Misrahi, M. The roles of luteinizing hormone, Follicle-Stimulating hormone and testosterone in spermatogenesis and folliculogenesis revisited. *Int. J. Mol. Sci.* **22**, (2021).
27. Santi, D. et al. Follicle-stimulating hormone (FSH) action on spermatogenesis: A focus on physiological and therapeutic roles. *J. Clin. Med.* **9**, (2020).
28. Smith, L. B. & Walker, W. H. The regulation of spermatogenesis by androgens. *Semin Cell. Dev. Biol.* **30**, 2–13 (2014).
29. Naamneh Elzenaty, R., du Toit, T. & Flück, C. E. Basics of androgen synthesis and action. *Best Pract. Res. Clin. Endocrinol. Metab.* **36**, 101665 (2022).
30. Gao, J., Qin, Y. & Schimenti, J. C. Gene regulation during meiosis. *Trends Genet.* **40**, 326–336 (2024).
31. Neto, F. T. L., Bach, P. V., Najari, B. B., Li, P. S. & Goldstein, M. Spermatogenesis in humans and its affecting factors. *Semin Cell. Dev. Biol.* **59**, 10–26 (2016).
32. Eto, K., Shiotsuki, M. & Abe, S. I. Nociceptin induces Rec8 phosphorylation and meiosis in postnatal murine testes. *Endocrinology* **154**, 2891–2899 (2013).
33. Burton, K. A. & McKnight, G. S. PKA, germ cells, and fertility. *Physiol. (Bethesda)*. **22**, 40–46 (2007).
34. Liang, Z. et al. AKAP3-mediated type I PKA signaling is required for mouse sperm hyperactivation and fertility†. *Biol. Reprod.* **110**, 684–697 (2024).
35. Yamamoto, C. et al. The cAMP signaling module regulates sperm motility in the liverwort *Marchantia polymorpha*. *Proc. Natl. Acad. Sci. U S A*. **121**, e2322211121 (2024).
36. Dey, S., Brothag, C. & Vijayaraghavan, S. Signaling enzymes required for sperm maturation and fertilization in mammals. *Front. Cell. Dev. Biol.* **7**, 341 (2019).
37. Huang, J. C. et al. HB-EGF induces mitochondrial dysfunction via Estrogen hypersecretion in granulosa cells dependent on cAMP-PKA-JNK/ERK-Ca(2+)-FOXO1 pathway. *Int. J. Biol. Sci.* **18**, 2047–2059 (2022).
38. Signorile, A. et al. cAMP/PKA signaling modulates mitochondrial supercomplex organization. *Int. J. Mol. Sci.* **23**, (2022).
39. Boyman, L., Karbowski, M. & Lederer, W. J. Regulation of mitochondrial ATP production: Ca(2+) signaling and quality control. *Trends Mol. Med.* **26**, 21–39 (2020).
40. Althaher, A. R. & Alwahsh, M. An overview of ATP synthase, inhibitors, and their toxicity. *Heliyon* **9**, e22459 (2023).
41. Guo, C. et al. ClpP/ClpX deficiency impairs mitochondrial functions and mTORC1 signaling during spermatogenesis. *Commun. Biol.* **6**, 1012 (2023).
42. Radaelli, E. et al. Mitochondrial defects caused by PARL deficiency lead to arrested spermatogenesis and ferroptosis. *Elife* **12**, (2023).
43. Wang, Y. et al. Exposure to phenanthrene affects oocyte meiosis by inducing mitochondrial dysfunction and Endoplasmic reticulum stress. *Cell. Prolif.* **56**, e13335 (2023).
44. Zhang, L. et al. Mitochondrial Ca(2+) overload leads to mitochondrial oxidative stress and delayed meiotic resumption in mouse oocytes. *Front. Cell. Dev. Biol.* **8**, 580876 (2020).
45. Zhang, L. Y. et al. Mitochondrial calcium uniporters are essential for meiotic progression in mouse oocytes by controlling Ca(2+) entry. *Cell. Prolif.* **54**, e13127 (2021).

Acknowledgements

This work was supported by the National Natural Science Foundation of China (81671625 and 81100554), the Young and Middle-Aged Scientists Research Awards Fund of Shandong Province(BS2012YY003), the Scientific and Technical Development Project of the Department of Health of Shandong Province(2011QZ007 and 2016WS0259), Shandong Province Natural Science Fund Project(ZR2014HM015), Project of Shandong Province Higher Educational Science and Technology Program (J14LK11) and the Scientific and Technical Development Project of Qingdao (12-1-4-20-jc, 2013-13-008-YY and 17-3-3-15-nsh).

Author contributions

Jiaojiao Qi (First Author): Conceptualization, Data Curation, Formal Analysis, Investigation, Methodology, Software, Visualization, Writing-Original Draft, Writing-Review & Editing; Yu Sun and Zeqing Chen: Methodology, Supervision; Shichao Xing(Corresponding Author): Conceptualization, Funding Acquisition, Resource, Supervision, Validation, Writing-Original Draft, Writing-Review & Editing; Ruipeng Gao, Shang Wang, Qing Zhang, and Xuelin Gong: Supervision, Validation; Miao Song, Tong Zou and Chengyang Liu: Data Curation, Investigation. We confirm that this work is original and has not been published previously, nor is it currently under consideration for publication elsewhere. All contributing authors have reviewed this manuscript.

Declarations

Competing interests

The authors declare no competing interests.

Ethics statement

Animal research was approved by the Affiliated Hospital of Qingdao University (Approval code: AHQU-MAL20230322) and was performed in line with the principles of the Declaration of Helsinki.

Additional information

Supplementary Information The online version contains supplementary material available at <https://doi.org/10.1038/s41598-025-95846-6>.

Correspondence and requests for materials should be addressed to S.X.

Reprints and permissions information is available at www.nature.com/reprints.

Publisher's note Springer Nature remains neutral with regard to jurisdictional claims in published maps and institutional affiliations.

Open Access This article is licensed under a Creative Commons Attribution-NonCommercial-NoDerivatives 4.0 International License, which permits any non-commercial use, sharing, distribution and reproduction in any medium or format, as long as you give appropriate credit to the original author(s) and the source, provide a link to the Creative Commons licence, and indicate if you modified the licensed material. You do not have permission under this licence to share adapted material derived from this article or parts of it. The images or other third party material in this article are included in the article's Creative Commons licence, unless indicated otherwise in a credit line to the material. If material is not included in the article's Creative Commons licence and your intended use is not permitted by statutory regulation or exceeds the permitted use, you will need to obtain permission directly from the copyright holder. To view a copy of this licence, visit <http://creativecommons.org/licenses/by-nc-nd/4.0/>.

© The Author(s) 2025